ISME

www.nature.com/ismej

ARTICLE

Conjugative transfer of streptococcal prophages harboring antibiotic resistance and virulence genes

Jinhu Huang[1,8], Xingyang Dai[1,8], Zuowei Wu[2,8], Xiao Hu[2], Junjie Sun[1], Yijun Tang[3,4], Wanqiu Zhang[3,4], Peizhao Han[1], Jiaqi Zhao[1], Guangjin Liu[5], Xiaoming Wang[1], Shengyong Mao[3,4], Yang Wang[6], Douglas R. Call[7], Jinxin Liu[3,4]✉ and Liping Wang[1]✉

Prophages play important roles in the transduction of various functional traits, including virulence factors, but remain debatable in harboring and transmitting antimicrobial resistance genes (ARGs). Herein we characterize a prevalent family of prophages in *Streptococcus*, designated SMphages, which harbor twenty-five ARGs that collectively confer resistance to ten antimicrobial classes, including *vanG*-type vancomycin resistance locus and oxazolidinone resistance gene *optrA*. SMphages integrate into four chromosome attachment sites by utilizing three types of integration modules and undergo excision in response to phage induction. Moreover, we characterize four subtypes of Alp-related surface proteins within SMphages, the lethal effects of which are extensively validated in cell and animal models. SMphages transfer via high-frequency conjugation that is facilitated by integrative and conjugative elements from either donors or recipients. Our findings explain the widespread of SMphages and the rapid dissemination of ARGs observed in members of the *Streptococcus* genus.

The ISME Journal (2023) 17:1467–1481; https://doi.org/10.1038/s41396-023-01463-4

INTRODUCTION

Prophages are temperate phages that are either integrated into the bacterial chromosome or maintained extra-chromosomally as episomes [1, 2]. They play crucial roles in mediating bacterial pathogenicity by secreting virulence factors (VFs), such as toxins, adhesins, and effector proteins [3–6]. Prophages are reported to harbor antimicrobial resistance genes (ARGs) [7, 8]; however, several recent bioinformatic studies demonstrated that identifying phage-sourced ARGs is sometimes "artificial" by relaxing the detection limits, and in fact, phages rarely encode clinically relevant ARGs [9, 10]. ARGs residing on the bacterial genomes can also be transferred by phage-mediated general transduction [11, 12], but the probability of such movement remains relatively low, due to the fact that bacterial DNA is randomly encapsulated by phage particles and the encapsulated DNA, if any, typically lysogenizes at low rates [13]. Together, the role of prophages in harboring and transmitting ARGs in natural ecosystems remains debatable.

Antibiotic-resistant streptococci severely compromise the clinical treatments with existing antibiotics, of which multidrug-resistant *S. pneumoniae*, erythromycin-resistant *S. pyogenes*, and clindamycin-resistant *S. agalactiae* frequently cause human infections [14, 15] and are included in the U.S. Centers for Disease Control and Prevention's 2019 antibiotic resistance threats list [16]. In addition, *S. suis*, a reservoir of clinically important ARGs for major streptococcal pathogens [17, 18], are considered as one emerging multidrug-resistant zoonotic pathogen [14]. In these *Streptococcus* species, the acquisition of antibiotic resistance is largely facilitated through the horizontal gene transfer (HGT) of ARG-carrying mobile genetic elements (MGEs), primarily integrative and conjugative elements (ICEs), integrative and mobilizable elements (IMEs), and the recently emerged prophages [19–24]. ICEs are self-transmissible mosaic and modular MGEs primarily residing in the bacterial host chromosome. ICEs encode the conjugation machinery not only for their self-transfer but also to mobilize other MGEs, including IMEs and genomic islands [25, 26]. IMEs encode the recombination module, allowing them to integrate into and excise from bacterial attachment sites. However, they carry only some sequences or genes necessary for their conjugative transfer [27]. Prophage-mediated transfer is known to occur mainly through generalized, specialized and lateral transduction [28–30]. However, non-classical transfer mechanisms have been characterized, involving transformation of DNA upon lysis by "superspreader" bacteriophage [31], as well as being mobilized via auto-transduction [32]. Although a list of classical and non-canonical HGT mechanisms have been characterized, the presence of unrecognized mechanisms of HGT mediated by MGEs is proposed [33], particularly the coordination

[1]MOE Joint International Research Laboratory of Animal Health and Food Safety, College of Veterinary Medicine, Nanjing Agricultural University, Nanjing 210095, China. [2]Department of Veterinary Microbiology and Preventive Medicine, College of Veterinary Medicine, Iowa State University, Ames, IA 50011, USA. [3]Ruminant Nutrition and Feed Engineering Technology Research Center, College of Animal Science and Technology, Nanjing Agricultural University, Nanjing 210095, China. [4]Laboratory of Gastrointestinal Microbiology, Jiangsu Key Laboratory of Gastrointestinal Nutrition and Animal Health, National Center for International Research on Animal Gut Nutrition, College of Animal Science and Technology, Nanjing Agricultural University, Nanjing 210095, China. [5]Key Lab of Animal Bacteriology, Ministry of Agriculture, OIE Reference Lab for Swine Streptococcosis, College of Veterinary Medicine, Nanjing Agricultural University, Nanjing 210095, China. [6]Beijing Advanced Innovation Center for Food Nutrition and Human Health, College of Veterinary Medicine, China Agricultural University, Beijing 100193, China. [7]Paul G. Allen School for Global Health, Washington State University, Pullman, WA 99164, USA. [8]These authors contributed equally: Jinhu Huang, Xingyang Dai, Zuowei Wu. ✉email: jxnliu@njau.edu.cn; wlp71@163.com

Received: 19 February 2023 Revised: 6 June 2023 Accepted: 16 June 2023
Published online: 27 June 2023

between phages and ICEs. Consequently, it remains unclear whether phages can transfer by "helper" ICEs for high-efficiency conjugation and vice versa.

Herein we systematically examined 10,983 public genomes in GenBank and 736 lab-owned isolates in *Streptococcus* and characterized a prevalent family of streptococcal mobilizable prophages, designated SMphages. This family of prophages encodes twenty-five ARGs (e.g., *vanG*-type vancomycin resistance locus and oxazolidinone resistance gene *optrA*) collectively conferring resistance to ten distinct classes of antimicrobial agents (e.g., vancomycin and oxazolidinones) and VFs belonging to four subtypes of Alp-related surface proteins (Alp-Ps). We present evidence that the transfer of SMphages occurs through both low-frequency transformation and high-frequency conjugation that is facilitated by co-resident ICEs from either donors or recipients. This mechanism of conjugation largely weakens the boundaries of distinct MGEs and opens a new door for the coordination of phages and ICEs in HGT.

RESULTS

SMphages are widely distributed in *S. agalactiae* and *S. suis*

We examined 10,983 public streptococcal genomes in GenBank and 736 lab-owned isolates from the National Antimicrobial Resistance Monitoring and Surveillance Program in Animals of China by a bidirectional strategy for the presence of ARG-associated prophages (Supplementary Fig. S1A, B). Although prophages from *Streptococcus* have been frequently detected [17], and are assumed to have a narrow host range [34], we found that ARGs were restricted to be carried by a unique family of prophages with a broad host range, which shares high sequence similarity to Φm46.1 [35] and Φ10394.4 [36] in *S. pyogenes*, λSa04 in *S. agalactiae* [37], and ΦSsUD.1 in *S. suis* [38]. These prophages, hereafter renamed as SMphages, were distributed in 21 *Streptococcus* species particularly *S. agalactiae* (47.0%, 455/969) and *S. suis* (8.9%, 124/1,399), but were absent in 12 *Streptococcus* species including *S. pneumoniae* (0/7,640) and *S. mutans* (0/174) (Supplementary Fig. S1C, D). The Φm46.1 regarding with ARGs was initially described and thought to be widespread in *S. pyogenes* [35, 39]; however, it was found to be present in only 1.17% of the examined *S. pyogenes* genomes (Supplementary Fig. S1C, D). By examining the attachment sites and the presence of ARGs or VFs, a total 253 SMphages (including the four previously reported prophages) from 244 *Streptococcus* strains were included in our subsequent analysis (Supplementary Fig. S1E and Supplementary Table S1).

Forty-five genes (*orf13-orf57*), approximately 38 kb in size, represent the core of SMphages (Fig. 1A), including five conserved functional modules (DNA replication, DNA modification, DNA packaging and morphogenesis, host cell lysis, and lysogeny control) as described in *Siphoviridae* [35, 38]. Adding two variable regions (VR1 and VR2), the majority (75%) of SMphages range between 49 and 60 kb in size depending on the host species and the attachment sites (Supplementary Fig. S1F), which likely represents the physical capacity that the capsid can accommodate [40]. Our phylogenetic analysis classified the prophage core genomes into the Clade_Sag (the *S. agalactiae* dominant subgroup) and the Clade_Ssu (the *S. suis* dominant subgroup) (Fig. 1B). SMphages from other species, for example, Φm46.1 of *S. pyogenes* and ΦSdyDY107_SAG0725 of *S. dysgalactiae*, were clustered into the Clade_Sag or Clade_Ssu subgroup, respectively (Fig. 1B).

SMphages are reservoir of clinically important ARGs

We identified twenty-five ARGs conferring resistance to ten classes of clinically relevant antibiotics in the VRs of SMphages (Fig. 1B and Supplementary Table S1), although the fact that most of these prophages harbor only a subset of these detected ARGs. These include macrolides-lincosamides-streptogramin B [*mef*(A), *msr*(D), *erm*(A), *erm*(B), *lnu*(B), *lnu*(C) and *lnu*(D)], tetracyclines [*tet*(M), *tet*(O), *tet*(W), tet(O/W/32/O), *tet*(40) and *tet*(44)], aminoglycosides [*ant(6)-Ib*, *ant(9')-Ia*, *aph(3')-IIIa*, *sat4*, *aadE* and *aac(6')-Ie-aph(2")-Ia*], phenicols-oxazolidinones [*catQ*, cat_{PC194} and *optrA*], pleuromutilins [*lsa*(E)], vancomycin [*vanG*-type locus], and trimethoprim [*dfrG*]. The most prevalent ARGs carried by prophages were the macrolides-lincosamides-streptogramin B resistance genes *erm*(B) (18.18%, 46/253), *mef*(A) (14.23%, 36/253) and *msr*(D) (12.25%, 31/253), the aminoglycosides resistance gene *aadE* (17.79%, 45/253), the tetracyclines resistance gene *tet*(M) (17.39%, 44/253), and the phenicols-oxazolidinones resistance gene *optrA* (7.91%, 20/253). Resistance phenotypes were validated by conventional minimum inhibitory concentration (MIC) assays in clinical isolates (Supplementary Table S1).

Analysis of the SMphage genomes revealed the presence of a variety of ARG-carrying fragments, including the IQ module, which carried the *mef*(A)-*msr*(D)-*catQ* that confers macrolides and chloramphenicol resistance phenotype and was first identified in *S. pneumoniae* (Fig. 2A), the *tet*(44) and *ant(6)-Ib* carrying fragments (Fig. 2B), the *aac(6')-aph(2")*-carrying fragments (Fig. 2C), the *optrA*- and *lnu*(C)-carrying fragments (Fig. 2D), the *vanG*-type locus (Fig. 2E), and the *dfrG*- and *lsa*(E)-*lnu*(B)-carrying fragments (Fig. 2F), in VR1 or VR2 of the Clade_Ssu subgroup, and the insertion of *tet*(M)-carrying Tn916 (~18 kb) and *tet*(M)-*erm*(B)-carrying Tn916-like (~23 kb) elements in the Clade_Sag subgroup SMphages (Supplementary Fig. S2A), highlighting that the VRs of SMphages are insertion hotspots for ARG-carrying fragments. Of particular concern, vancomycin and oxazolidinones are among the first-line and last-resort antimicrobial agents in treating multidrug-resistant Gram-positive bacterial infections, and the accumulation of *vanG*-type vancomycin resistance locus and oxazolidinone resistance gene *optrA* within SMphages may facilitate the transfer of these ARGs to other Gram-positive bacteria [41]. In addition, a chimeric macrolide efflux genetic assembly (Mega)-like element, consisting of a Mega element carrying *mef*(A)-*msr*(D), which confers a macrolides phenotype, and an *orf5-orf6-umuC-orf8-hdiR* operon, which is thought to mediate SOS mutagenesis [42], was widely distributed in SMphages from multiple species (Supplementary Fig. S2B). Importantly, our tanglegram analysis revealed the presence of nearly identical SMphages (>90% coverage with >90% identity) in distinct *Streptococcus* species, indicating extensive HGT of SMphages between strains *Streptococcus* species (Fig. 1B and Supplementary Fig. S3).

SMphages integrate and excise by recognizing a previously undescribed 8-bp motif

Integrase is typically required for the site-specific integration and excision of prophages from bacterial chromosomes. For these 253 SMphages, integration mainly occurred at one of the following four *attB* sites: 1) 3′-end of *rum* in 13 species, a well-conserved housekeeping gene encoding a 23 S rRNA uracil methyltransferase [17, 43]; 2) the middle of *comEC* in seven species, one of the major components of DNA uptake apparatus for transformation [44, 45]; 3 and 4), the remaining two novel loci, 5′-start of *SAG0725* and *SAG1105* in six species, both genes encoding a haloacid dehalogenase family hydrolase (Fig. 3A). Consistent with this data, our phylogenetic analysis classified the two serine integrase genes of SMphages, *intI* (*orf56*, internal) and *intE* (*orf57*, external), into three clusters associated with *attB* sites: *rum*, *comEC*, and *SAG0725/SAG1105* (Fig. 3B). Some prophages with the same IntIE types scattered into distinct subgroups of SMphages while others with different IntIE types clustered together into the same subgroups of SMphages (Fig. 1B), indicating a recent module exchange of IntIE modules. These findings suggest that SMphages can exploit a diverse type of integration/excision modules, which likely contribute to the integration diversity in *Streptococcus*.

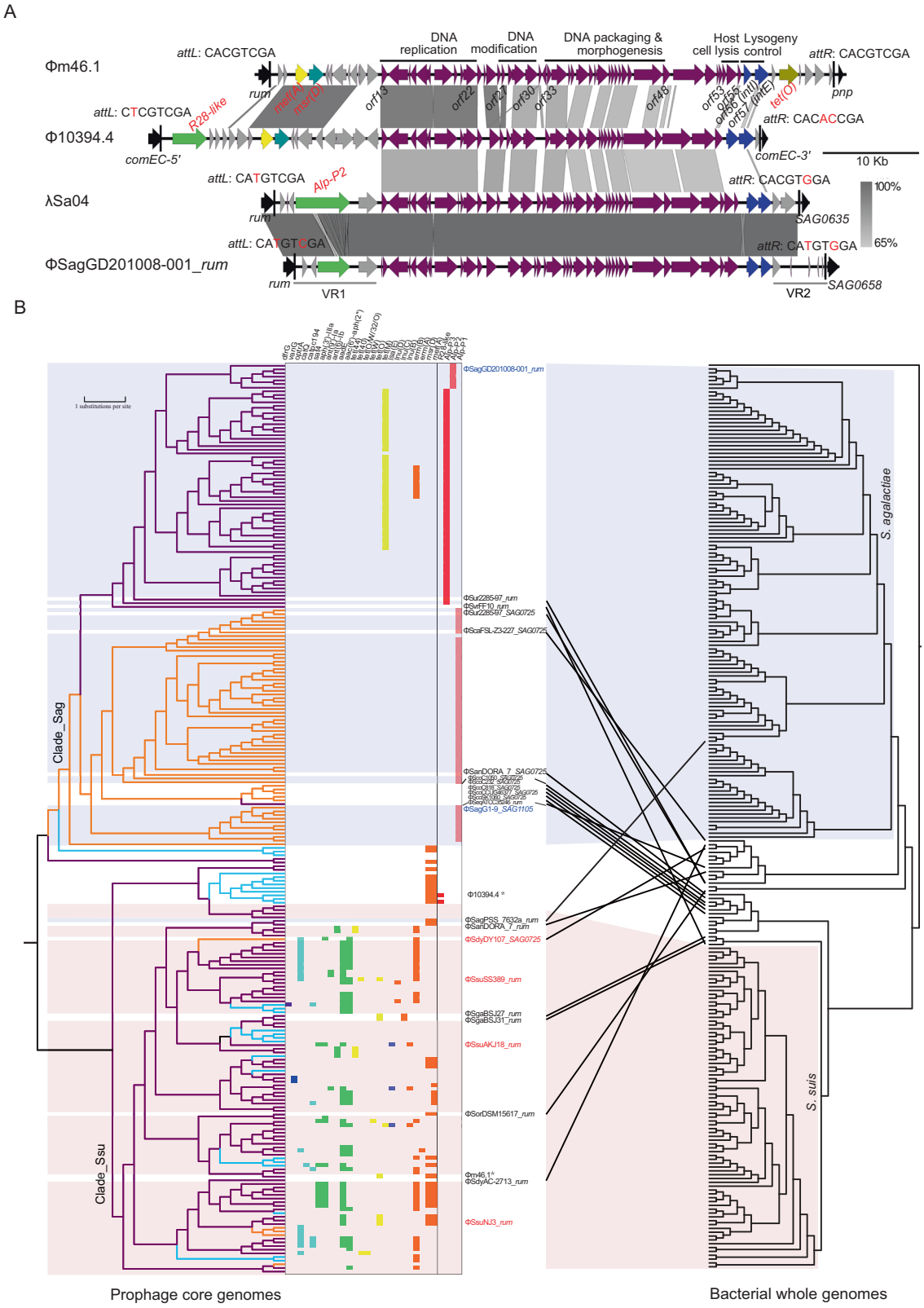

When integration occurs, phage integrases recognize two attachment sites in phage (*attP*) and bacteria (*attB*) and generate two new hybrid sequences termed *attL* and *attR*. SMphages were thought to recognize a 2-bp GA motif when integrating at *rum* site in previous study [46]. In contrast, we systematically examined SMphages at all four *attB* sites (Fig. 3C, D) and identified an 8-bp imperfect match sequence depending on their IntIEs and *att* sites. SMphages with the $IntIE_{rum}$ module integrate into the up-stream region of the 8-bp *attB* sequence, generating a hybrid *attL*/*attP* and *attR*/*attB* sequence, while SMphages with $IntIE_{comEC}$ or

Fig. 1 SMphage organization and prophage-host crosstalk inferred by phylogenetic analysis of SMphage and bacterial genomes. **A** Organization of representative SMphages. The core genes *orf13-orf55* and *orf56-orf57* are indicated by purple and blue arrows, respectively. The accessary genes are flanked into two variable regions (VR1 and VR2) and indicated by grey arrows with ARGs and Alp-Ps colored by different colors. Putative attachment sequences were identified on the left (*attL*) and right (*attR*) border. **B** (Left panel) A prophage phylogenetic tree was constructed from 253 SMphages core genomes *orf13-orf55*. Branches were colored by *attB* sites: purple, *rum* site; light blue, *comEC* site; dark orange, *SAG0725/SAG1105* site. The distribution of ARGs and four subtype Alp-Ps were presented (detailed in Supplementary Table S1). (Right panel) A bacterial whole genome phylogenetic tree was constructed from 244 bacterial genomes that carried SMphages. SMphages from *S. agalactiae* and *S. suis* were shadowed in light grey and light pink, respectively. Connect lines indicate potential interspecific transfer of SMphages. Prophages that were previously reported are marked with asterisk and SMphages used for HGT and virulence studies are highlighted in red and blue, respectively.

IntIE$_{SAG0725/SAG1105}$ module integrate into the down-stream region of *attB*, generating hybrid *attL*/*attB* and *attR*/*attP* sequences (Fig. 3E, F).

Horizontal transfer of SMphages is assisted by ICEs via high-efficiency conjugation

In the genus *Streptococcus*, phage-mediated transfer and lysogenisation is considered to occur at relatively low frequency within a narrow host range in previous study [28]. Because SMphages were widely present across *Streptococcus* species and our above tanglegram analysis indicates the extensive intraspecific and interspecific HGT, we inferred the presence of novel mechanism(s) might be involved, permitting relatively high frequency HGT for SMphages. To test this hypothesis, we designed a set of transfer assays to identify the prophage HGT mechanisms by transduction, transformation, or conjugation (Fig. 4A). Four isolates harboring SMphages were selected as donors for transfer assays, including two ICE-negative strains (*S. suis* NJ3 and *S. suis* SS389) and two ICE-positive strains (*S. dysgalactiae* DY107 and *S. suis* AKJ18) (Supplementary Fig. S4a and Supplementary Table S2). Phage particles were induced by mitomycin C (MMC) and purified from these four strains, with the typical icosahedral head and tail morphology of the *Siphoviridae* (Fig. 4B). The presence of DNase I-resistant SMphage genomes in phage particles was confirmed by PCR detection of prophage core module genes and related ARGs (data not shown). We next performed plaque and transduction assays using 45 clinical isolates as recipients (30 *S. suis* including *S. suis* P1/7RF, 10 *S. agalactiae*, and 5 *S. dysgalactiae*). However, positive plaque and lysogenic transfer were not observed after more than five attempts (data not shown). The failure of lysogenic transfer is likely the consequence of a low infecting phage titer, which is a common feature of prophages in group A *Streptococcus* [47]. These results suggested a limited role of this mechanism in HGT of SMphages and ARGs.

Considering that phage particle lysis or activation of autolysis can release free prophage DNA [48], we then examined the transferability of SMphages via transformation. Transformation was only successful between purified phage DNA from *S. suis* NJ3 and recipient *S. suis* strain P1/7RF, but at a low frequency and requiring a large mass (2 μg) of phage DNA (Fig. 4a). These data highlight that transformation does occur but the contribution is also minor in the HGT of SMphages and ARGs.

Conjugation was next assessed with filter mating assays using the above four donor strains (carrying SMphages) and the recipient strain *S. suis* P1/7RF. We found that SMphages from the four donors were all successfully transferred into the recipient, but the transfer frequency in ICE-positive strains (DY107 and AKJ18) was >400-fold higher than those in ICE-negative strains (NJ3 and SS389) (Fig. 4C). Given that the two ICE-negative donors did not have conjugative systems, the HGT of SMphages might be unrelated to conjugation. To further test this, the bacteria medium was pretreated by DNase I to remove the free donor DNA that might lead to the transfer by natural transformation (Fig. 4C). Consequently, the HGT of SMphages was abolished in ICE-negative strains NJ3 and SS389, in contrast to results from the ICE-positive strains DY107 and AKJ18 (Fig. 4C). These data highlight the important role of ICE in facilitating the intra- and inter-specific HGT of prophages via conjugation. We further validated the role of ICE in HGT of SMphages by deletion of ICE from the donor strain *S. suis* AKJ18 (AKJ18ΔICE) and by adding an ICE (ICE*Ssu*AKJ47_*SSU1797*) to the recipient strain P1/7RF (P1/7RF::ICE). AKJ18ΔICE abolished HGT of SMphages to the recipient strain P1/7RF (Fig. 4D and Table 1), and restored HGT to the recipient strain P1/7RF::ICE (Fig. 4D and Table 1). In addition, another ICE-negative strain NJ3 was further applied to mate with recipient P1/7RF::ICE, and HGT of SMphages was successfully observed (Fig. 4D and Table 1). These results confirmed that ICE-mediated conjugation is an important HGT mechanism of prophages in *Streptococcus* at high-frequency (~10^{-6}).

Southern blots experiments and complete genome sequencing of the transconjugants confirmed the transfer of ARGs-carrying SMphage DNA fragments into recipients (Supplementary Fig. S4B). For transconjugants cAKJ18 and cNJ3, the intact SMphages were site-specifically integrated into the same *attB* (*rum*) sites as in the donors, but the ΦSdyDY107_*SAG0725* was integrated into *SSU0237* (*SAG1105*) site in transconjugant cDY107 rather than the primary *attB* (*SAG0725*) site (Fig. 4E and Supplementary Fig. S4C). In addition, the prophage-carrying DNA segment in the transconjugant cSS389 underwent homologous recombination with the recipient chromosome to generate a large hybrid region consisting of two regions of ~50 kb and ~208 kb from the donor and an inversion region of ~260 kb from the recipient chromosome (Fig. 4F and Supplementary Fig. S4C).

The acquisition of SMphages in *Streptococcus* helps bacterial hosts gain functional traits. As expected, transconjugants were resistant to antibiotics corresponding to the ARGs carried by SMphages (Table 1). We used growth and competition assays to examine potential fitness costs associated with the acquisition of SMphages. Recipient strains were not adversely affected when acquiring ΦSdyDY107_*SAG0725* or ΦSsuAKJ18_*rum*, but growth was inhibited for ΦSsuNJ3_*rum* and growth was improved for ΦSsuSS389_*rum* (Supplementary Fig. S4D). Relative to wild-type recipient P1/7RF, there was a clear fitness cost for strain cNJ3 ($w = 0.878$) and a fitness benefit for strain cSS389 ($w = 1.13$) based on in vitro competition assays (Supplementary Fig. S4E). One possible reason might be the different accessory genes in VRs of different prophages (e.g., the different ARGs). However, the prophage integration into the attachment site or homologous recombination with bacterial host chromosomes may also alter the transcription of the host genes. Thus, prophage and host factors could be interesting candidates for studying their effects on bacterial fitness. SMphages in transconjugants functioned as expected including having an integrated prophage and spontaneously excised episome phenotype (Supplementary Fig. S5A), and mitomycin C treatment resulted in induced circularization of SMphages and the release of mature phage particles (Fig. 4B and Supplementary Fig. S5B–D). Since the recipient *S. suis* P1/7RF strain is negative for any prophage, the observation of phage particles in transconjugants further confirmed the transfer and integration of SMphages. However, plaques were not detected

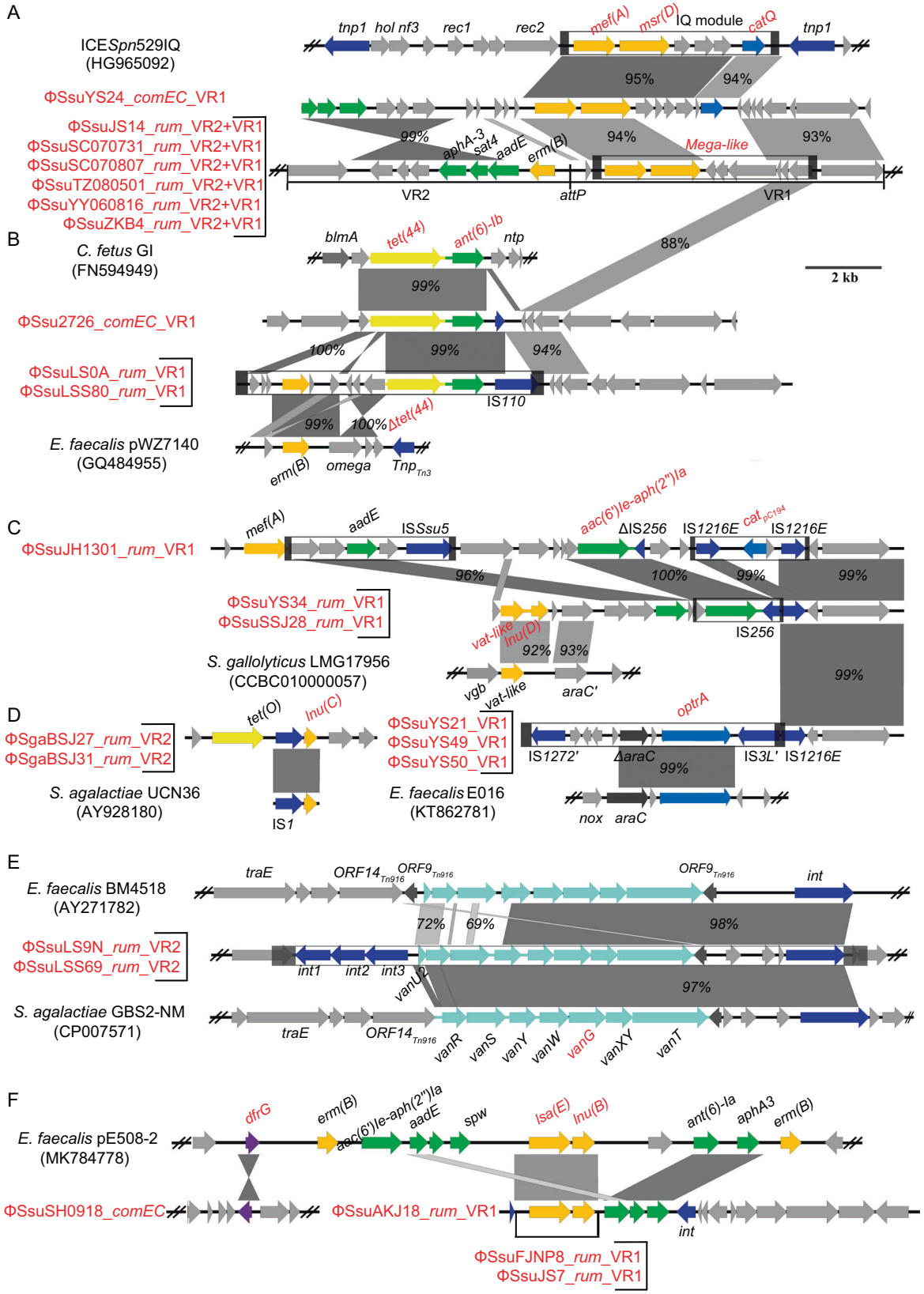

Fig. 2 ARG-carrying fragments accreted within VRs of Clade_Ssu subgroup SMphages. A Comparison of the IQ module and Mega-like elements. **B** Comparison of the *tet*(44)- and *ant(6)-Ib*-carrying fragments. **C** Comparison of different fragments that carried *aac(6')-Ie-aph(2")-Ia*. **D** Comparison of fragments that carried *lnu*(C) or *optrA* genes. **E** Comparison of the *vanG*-carrying fragments. **F** Comparison of the fragments that carried *dfrG*, *lnu*(B) and *lsa*(E).

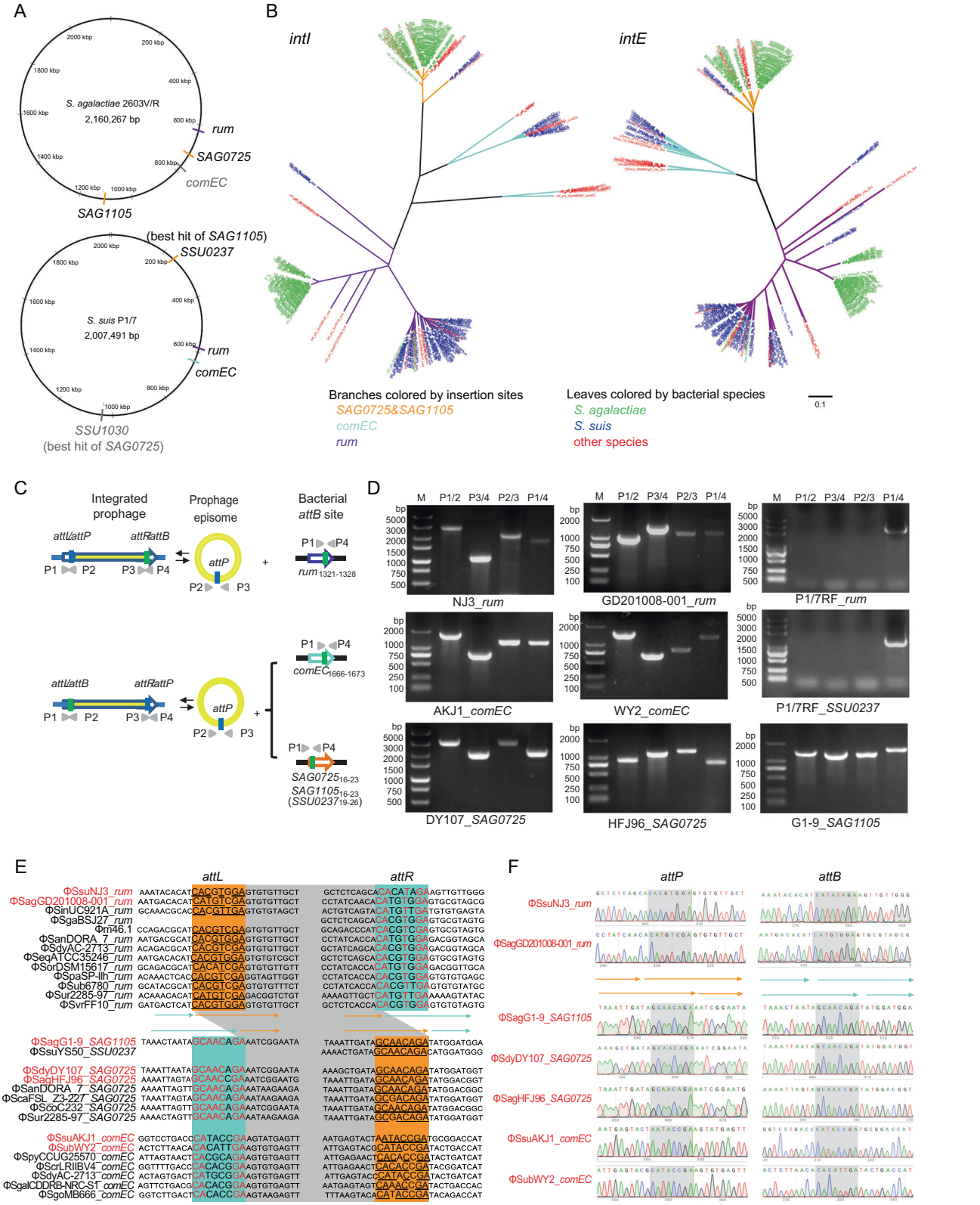

Fig. 3 Integration and excision of SMphages. A SMphage insertion locations within the host genomes. *S. agalactiae* 2603 V/R and *S. suis* P1/7 were used as reference genomes. **B** Phylogenetic analysis of integrase genes *intI* and *intIE* (*orf56-57* of Φm46.1). **C** Schematic diagram of SMphages integrated in and excised from host bacteria *attB* sites. **D** PCR amplification of the presence of both integrated form (*attL* and *attR*) and excised/episome form (*attB* and *attP*) of the SMphages. **E** Sequence analysis of the *attL* and *attR* sites of when SMphages integrated into host bacteria. **F** Sequence analysis of the *attP* and *attB* sites of when SMphages excised from host bacteria as phage episomes.

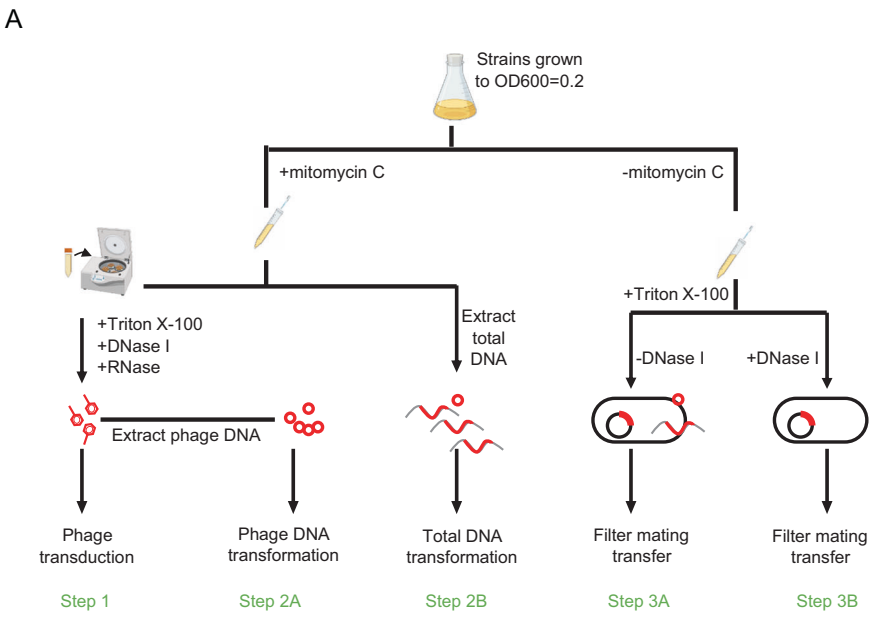

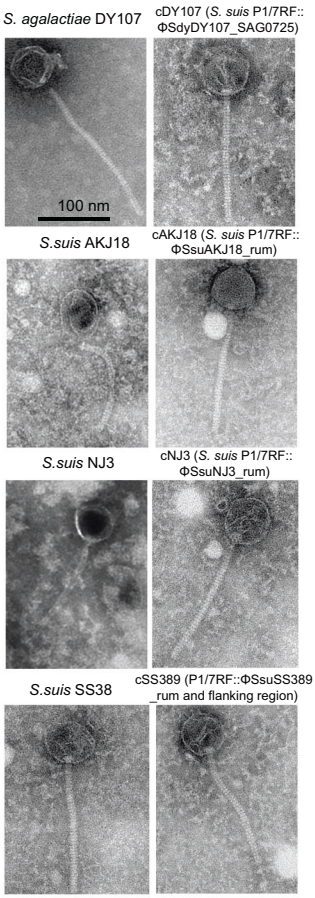

Strain	SMphage	2nd prophage	ICE	Step 1	Step 2A	Step 2B	Step 3A	Step 3B	HGT pathway
S. dysagalactiae DY107	*SAG0725*	*rplJ*	*rum*	–	NA	NA	+++	+++	conjugation
S. suis AKJ18	*rum*	*ssrA*	*rum*	–	NA	NA	+++	+++	conjugation
S. suis NJ3	*rum*	*comGA*	-	–	+	–	+	–	transformation
S. suis SS389	*rum*	*SSU1458*	-	–	–	–	+	–	transformation
S. suis P1/7RF		N		Used as recipient strain					

NA, Not Applicable; N, genative for prophages and ICEs.

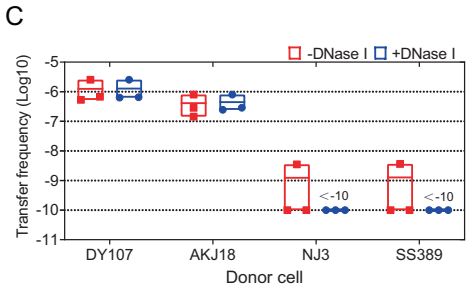

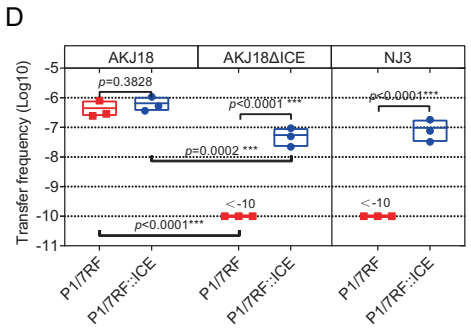

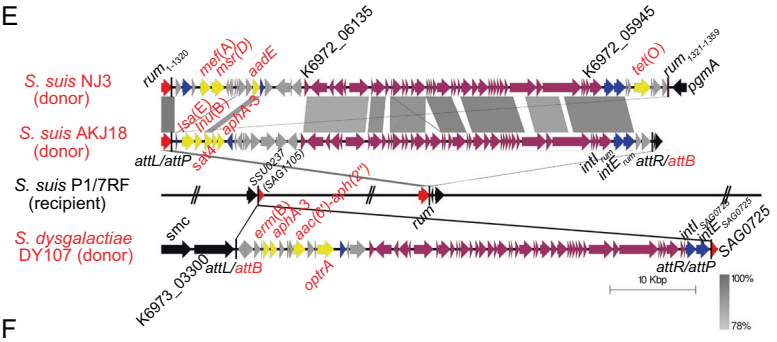

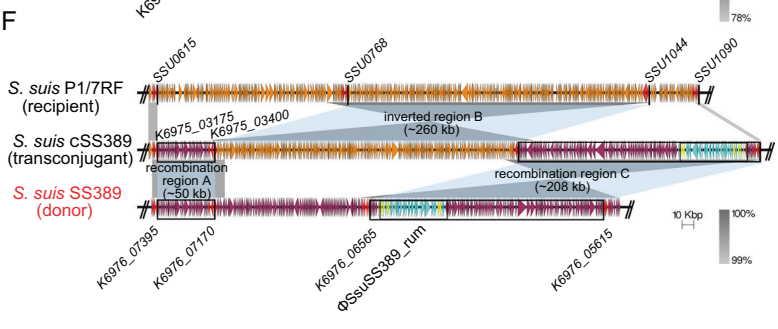

in transconjugants under these experimental conditions as in the case of donors.

Collectively, we confirmed that the intraspecific and interspecific transfer of SMphages occurs through both low-frequency transformation and high-frequency conjugation, after which SMphages integrated into the recipient bacterial chromosome through either site-specific or homologous recombination, thus altering bacterial fitness.

Fig. 4 HGT mechanisms of SMphages. A Experimental design to distinguish the HGT mechanisms by transduction, transformation, or conjugation. The information of strains and their HGT pathway was shown in the table. +++, >100 colonies/plate; +, 1 ~ 10 colonies/plate; -, no colonies on plates. **B** Electron microscopic images of phage particles purified from donors (left row) and transconjugants (right row) after prophage induction. **C** Transfer of SMphages in filter mating transfer assays (Step 3 in Fig. 4A). The ICE-positive strains DY107 and AKJ18 showed more than 400-folds higher frequency than ICE-negative strains NJ3 and SS389. In the presence of DNase I, HGT of SMphages was abolished in ICE-negative isolates but maintained in ICE-positive strains. **D** Conjugative transfer experiments included DNase I treatment to exclude nature transformation. Deletion of ICE in donor AKJ18 (AKJ18ΔICE) abolished HGT of SMphages to the recipient strain P1/7RF. The addition of ICE in recipient P1/7RF (P1/7RF::ICE) restored HGT in ICE-defective donor AKJ18ΔICE and ICE-negative strain NJ3. **E**, **F** Genetic comparison and integration of SMphages into recipient strain. ΦSsuNJ3_rum and ΦSsuAKJ18_rum were site-specific integrated into the *rum* site, while ΦSdyDY107_SAG0725 was site-specific integrated into *SSU0237* (*SAG1105*) site. For transconjugant cSS389, Region A (~50 kb) and Region C (~208 kb of the ΦSsuSS389_rum and flanking fragment) were homologously recombined from donor SS389 with an inversion region of ~260 kb from the recipient chromosome.

SMphage-encoded Alp-Ps enhanced the pathogenesis of *S. agalactiae*

Alp-related surface proteins are heavily involved in the pathogenesis of *S. agalactiae*, and are commonly used as targets for *S. agalactiae* vaccines [49, 50]. In addition, a homologous protein R28, which is identical to Alp3, was reported in *S. pyogenes* and contributed to virulence [51]. Beyond *S. pyogenes*, another Alp named Dys-Alp has also been reported in *S. dysgalactiae* subsp. *equisimilis* [52]. A previous study reported that a R28-like Alp related to Alp3 was carried by a *S. pyogenes* Φ10394.4 prophage [36], suggesting that prophages are involved in cross-species transfer of Alps and related proteins. Sequence analysis identified 127 LPxTG-motif containing Alp-related proteins in SMphages that were classified into the Clade_Sag subgroup (Supplementary Table S1). We further analyzed the sequences of Alp-related proteins and clustered them into three new classes, designated as Alp-P1, Alp-P2, and Alp-P3, in addition to R28-like Alps (Supplementary Fig. S6A, B). Each of the three new Alp-Ps possesses a 47-aa signal peptide and a conserved 34-, 63-, or 49-aa C-terminal cell wall anchoring region with an LPxTG motif, while the "R" repeat region and N-terminal region were divergent (Supplementary Fig. S6C, D). Alp-P1 was carried by SMphages integrated at *SAG1105/SAG0725* sites, while Alp-P2 and Alp-P3 were carried by SMphages integrated at the *rum* locus (Supplementary Fig. S2A).

We next verified the virulence of the Alp-Ps using both cell and animal models. Two clinical *S. agalactiae* strains were tested, including strain G1-9 (milk source from cow diagnosed with mastitis) with Alp-P1 in ΦSagG1-9_*SAG1105* and strain GD201008-001 (tilapia source with meningoencephalitis) [53] containing Alp-P2 in ΦSagGD201008-001_*rum*. Mutant strains with deletion Δ*alp*-P1 and Δ*alp*-P2 and with complement CΔ*alp*-P1 and CΔ*alp*-P2 were constructed, which did not compromise bacterial growth (Supplementary Fig. S7A). The Δ*alp*-P1 and Δ*alp*-P2 mutants exhibited a significant reduction in adhesion and invasion compared to both wild-type and complementary strains to bovine mammary epithelial cells (BMEC) and human larynx epidermoid carcinoma cells (HEp-2), respectively (Fig. 5A, B). In a zebrafish infection model, the Δ*alp*-P1 strain was attenuated relative to the wild-type ($p = 0.00081$, Fig. 5C) and the complemented strains (CΔ*alp*-P1, $p = 0.0012$, Fig. 5C), whereas the Δ*alp*-P2 strain was not attenuated ($p = 0.14$, Fig. 5C) at 120 h post-infection (Fig. 5C). In a mouse infection model, fewer Δ*alp*-P1 bacteria were recovered from the brain, liver, and spleen but not in blood (Supplementary Fig. S7B). In the mouse model, the Δ*alp*-P1 strain was not attenuated ($p = 0.14$, Fig. 4D) whereas the Δ*alp*-P2 strain was marginally attenuated ($p = 0.038$, Fig. 5D). Consequently, SMphage-carried Alp-Ps are involved in bacterial adhesion and invasion, which likely contribute to the bacterial disease in *Streptococcus* although the effects may vary between host species.

DISCUSSION

Phages play important roles in bacterial evolution because of their potential for HGT of genetic materials between microbes [54]. The concept is accepted that transduction of phage-encoded VFs is a major factor in bacterial pathogenesis [55], but the role that prophages played in the spread of ARGs is underestimated, partly because of the low probability of ARGs being located on phage genomes [9, 10, 56]. With the exponential growth of bacterial genomics from public databases, it becomes possible to re-examine the probability of prophages in carrying ARGs [57]. Enabled by new strategies for ARG-associated prophage identification, here we report an exception, the SMphages, that encode twenty-five ARGs conferring resistance to ten distinct classes of antibiotics and VFs belonging to four subtypes of Alp-Ps in streptococci. Our findings revealed that prophages could serve as a reservoir of ARGs that can be mobilized across bacterial species.

SMphages are disproportionally distributed in different species of *Streptococcus* and predominantly distributed in *S. agalactiae* and *S. suis*. In addition to bacterial host factors, the distribution of other MGEs might be counted. For instance, *S. agalactiae* and *S. suis* appear as the species containing the highest number of ICEs [24] and IMEs [58]. Moreover, the co-existence of ICEs and SMphages within the same strains has been documented in *S. agalactiae* and *S. suis* [17]. This may explain the wide distribution of SMphages in specific species as validated in this study for ICEs coordination. ARGs carriage of SMphages is strongly related to the antibiotics used. For instance, the most prevalent ARGs include macrolides-lincosamides-streptogramin B resistance genes *erm*(B), *mef*(A) and *msr*(D), the aminoglycosides resistance gene *aadE*, the tetracyclines resistance gene *tet*(M), and the phenicols-oxazolidinones resistance gene *optrA*, of which the macrolides, tetracyclines, aminoglycosides and phenicols are extensively used in veterinary medicine [18, 41], while macrolides and oxazolidinones are clinical important antibiotics for the treatment of streptococcal infections in human medicine. Nearly all SMphages of the Clade_Sag subgroup carried a subtype of Alp-Ps, of which the virulence of Alp-P1 and Alp-P2 was verified in both cell and animal models, which indicated the adaptive evolution of *S. agalactiae* in favor of adhesion and invasion of epithelial cells [59, 60]. Fortunately, the results showed that Alp-Ps and the majority of ARGs are rarely found in the same phages. Nevertheless, co-location of Alp-P3 with *tet*(M)-carrying elements and R28-like with *mef*(A)-carrying elements was observed in *S. agalactiae* and *S. pyogenes*, respectively (Supplementary Table. S1), posing an increased risk to public health [61].

SMphages use two serine family sitespecific recombinases IntIE to integrate themselves into bacterial chromosomes. One such element was the SCC*mec* (Staphylococcal Cassette Chromosome *mec*), which carries the cassette chromosome recombinase genes AB or C (*ccrAB* or *ccrC*), mediating the integration and excision of the SCC*mec* into and from the chromosome by specific recognition of a 2-bp GA motif at the 3′-end of the *rlmH* [62]. Previous analysis of Φm46.1 suggested a similar mechanism by recognizing a 2-bp GA motif at the 3′-end of the *rum* [35]. However, the analysis was simply based on comparisons of sequences that did not take the imperfect direct repeats into consideration. In this study, we expanded the integration diversity of SMphages by integrating them into four *attB* sites due to the equipment of different types of IntIE modules. We

Table 1. Characteristics of the strains for which SMphages successfully transferred.

Donor	Recipient	Transconjugant	MGEs [AMR genes] transferred	Transfer frequency [a] (mean ± SD) × 10^{-9}	MIC (mg/L) [b]					
					LZD	FFC	ERY	TET	TIA	GEN
	S. suis P1/7RF		-		0.5	≤0.5	≤0.12	2	0.5	4
S. dysgalactiae DY107		cDY107	ΦSdyDY107_*SAG0725* [*erm*(B), *optrA*, *aph*(3′)-*IIIa*, *aac*(6′)-*Ie-aph*(2″)-*Ia*]	1,249.1 ± 1,121.1	***4***	***32***	***>256***	2	0.5	***256***
S. suis AKJ18		cAKJ18	ΦSsuAKJ18_*rum* [*lsa*(E), *lnu*(B), *addE*, *sat4*, *aph*(3′)-*IIIa*]	410.7 ± 346.0	0.5	≤0.5	≤0.12	2	***64***	2
S. suis AKJ18ΔICE		-	-	0	-	-	-	-	-	-
S. suis NJ3		cNJ3	ΦSsuNJ3_*rum* [*mef*(A), *msr*(D), *aadE*, *tet*(O)]	1.2 ± 2.0	0.5	≤0.5	***4***	***16***	0.5	4
S. suis SS389		cSS389	ΦSsuSS389_*rum* and flanking region [*erm*(B), *optrA*, *tet*(O), *tet*(40), *aadE*, *aac*(6′)-*Ie-aph*(2″)-*Ia*]	1.2 ± 2.1	***2***	***16***	***>256***	***32***	0.5	***256***
	S. suis P1/7RF::ICE		ICE*Ssu*AKJ47_*SSU1797* [*optrA*] [c]		***8***	***32***	≤0.12	2	0.5	4
S. suis AKJ18		ICE_cAKJ18_1	ICE*Ssu*AKJ47_*SSU1797*+ΦSsuAKJ18_*rum*	650.6 ± 371.9	***8***	***32***	≤0.12	2	***64***	2
S. suis AKJ18ΔICE		ICE_cAKJ18_2	ICE*Ssu*AKJ47_*SSU1797*+ΦSsuAKJ18_*rum*	55.0 ± 36.1	***8***	***32***	≤0.12	2	***64***	2
S. suis NJ3		ICE_cNJ3	ICE*Ssu*AKJ47_*SSU1797*+ΦSsuNJ3_*rum*	96.4 ± 76.4	***8***	***32***	***4***	***16***	0.5	4

[a]Transfer frequency was calculated based on the number of observed transconjugants divided by the initial number of donors in each assay of three duplicates.
[b]LZD, linazolid; FFC, florfenicol; ERY, erythromycin; TET, tetracycline; TIA, tiamulin; GEN, gentamicin. MICs in bolditalics represent resistance to corresponding antimicrobials according to CLSI M100-ED29 [68].
[c]*S. suis* P1/7RF::ICE was derived from P1/7RF by acquisition of an *optrA*-carrying ICE from *S. suis* AKJ47 using a conjugation assay.

then evaluated the integration and excision process of SMphages at all four *attB* sites from clinical isolates and compared the integration of SMphages before and after transfer into recipient/transconjugant cells. which identified that IntIEs recognize an 8-bp imperfect match direct repeat motif. In addition, the integration direction seems to depend on the IntIE types (Fig. 3E, F). In addition, the IntIEs of SMphages were continuously expressed at low transcriptional level even without exogenous stress, which allowed the spontaneous excision of SMphages to become "plasmid-like" episomes. Upon mitomycin treatment, the expression of IntIE was increased, which led to the excision of prophages followed by lytic production. Unlike SCC*mecs*, which do not encode transduction machinery for self-transfer but exploit the capsids of other phages (known as helper phages) for their transduction at high frequency [63], the SMphages encode intact transduction machinery for self-transfer, although the transduction occurred at extremely low frequency [28].

We demonstrate here that intra- and inter-specific HGT of SMphages is mediated by ICEs at a much higher frequency than transduction and transformation. Conjugation is predicted to be the preponderant mechanism of HGT between distant lineages [64]. ICEs represent the most abundant conjugative elements that carry the genes necessary for their own integration, excision, and the conjugation process [24, 64]. Despite transferring their own DNA, ICEs can also mobilize other MGEs, including IMEs, mobilizable genomic islands (MGIs), non-conjugative plasmids, and large genomic DNA fragments [26, 33]. These elements may exploit ICEs' conjugation machinery for their mobilization through either their own or ICE-encoded Relaxase that recognize the cognate origin of transfer (*oriT*) or *oriT* mimicry presented on the elements [26]. This is consistent with findings about MGIs in *Vibrio* species, where the SXT/R391 family's ICE-encoded MobI and putative Relaxase recognize $oriT_{MGI}$ to mobilize MGIs' transfer in trans to the recipient cells [65, 66]. However, whether ICEs can mobilize prophage genomes are still unknown. By construction of the ICE deletion and complement strains in both donor and recipient trains, we characterized a novel and efficient HGT mechanism for the conjugative transfer of SMphage genomes by ICEs from either donors or recipients. These findings represent a final piece of the puzzle that MGEs utilize each other's transfer machinery for their own HGT. The ICE encoded by either the donor or the recipient strains drive the conjugative transfer of prophage genomes at high frequency, which might explain the increasing prevalence of the prophages along with the dissemination of ICEs in *Streptococcus* species [17, 67]. However, SMphages lack a reported *relaxase* gene or a "mimic" of the ICE *oriT* sequence, which is required for mobilization by ICE via conjugation. The underlining mechanisms of how prophages exploit an ICE's conjugation machinery for their own mobilization remain to be discovered.

In summary, we show that prophages are reservoirs of clinically relevant ARGs and VFs and are distributed in many species of *Streptococcus*. Integration of SMphages into the bacterial chromosome occurs via either site-specific or homologous recombination. Integrated SMphages can be excised as episomes and such excision is readily inducible. Furthermore, SMphages employ multiple non-transduction HGT mechanisms in the dissemination of ARGs and VFs, including transformation at low frequency, and a previously undescribed conjugation mechanism at high frequency that is facilitated by ICEs from either donor or recipient cells. The "plasmid-like" lifestyle of SMphage whereby it is excised as an episome rather than a phage particle enables the mobilization of the phage genomes by coexisting ICE, which largely weakens the boundaries of different MGEs and opens a new broad perspective on how phages can contribute to the evolutionary change of bacteria with the help of ICEs. This novel HGT mechanism may explain the increasing prevalence of ICE-associated SMphages in *Streptococcus* and provides a basis for future studies of prophage mobilization in other bacterial taxa.

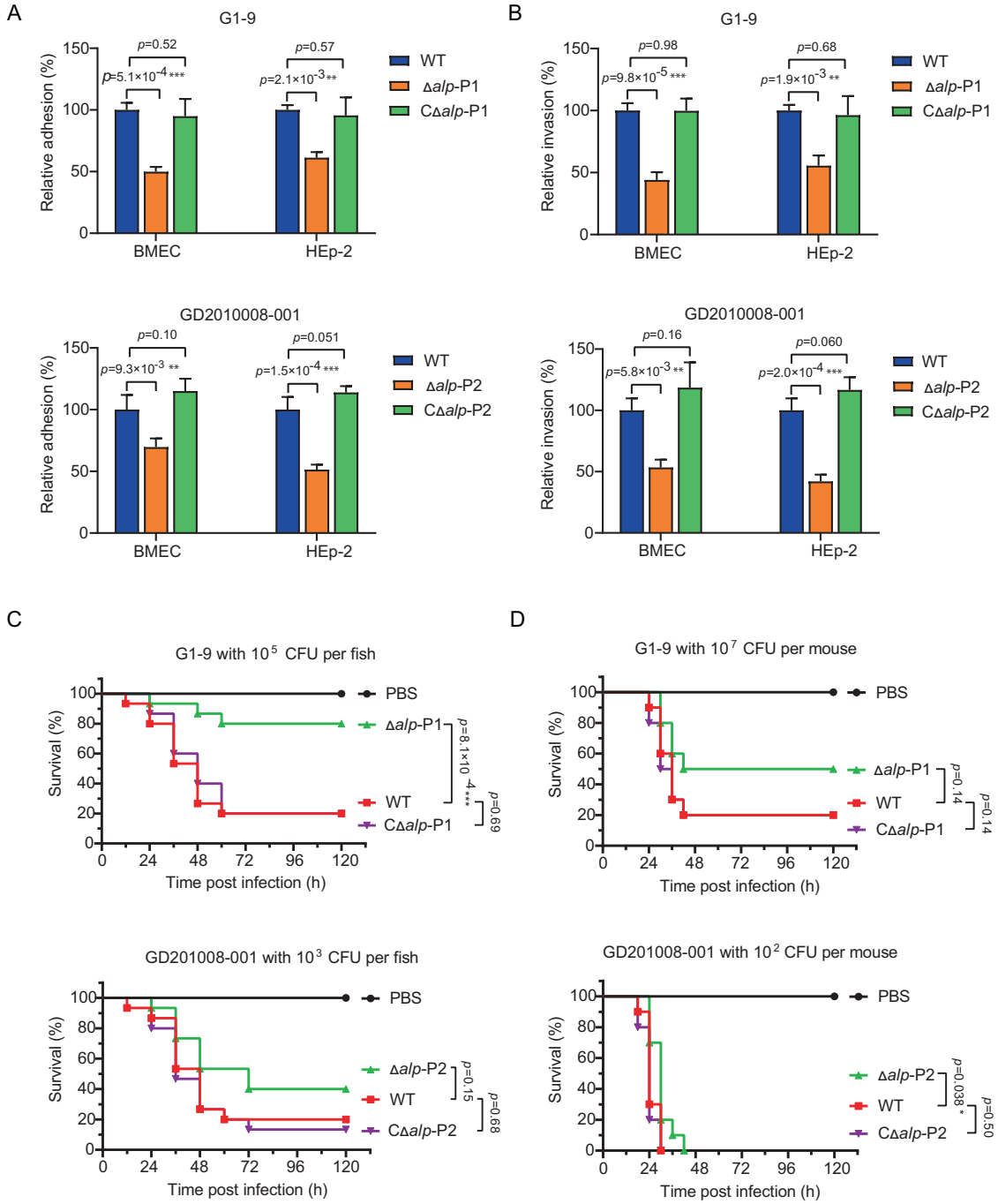

Fig. 5 Alp-Ps of Clade_Sag subgroup SMphages contributed to bacterial virulence to bacterial host. Role of Alp-P1 and Alp-P2 in relative adhesion (**A**) and invasion (**B**) levels to BMEC and HEp-2 cells at MOI of 1:100 after 2 h co-incubation. Bars represent the mean ± SD from three independent experiments. **C** Survival curve in a zebrafish infection model. The survival rate was recorded from triplicate experiments with 15 zebrafish in each group over a 120-h period. **D** Survival curve in a mouse infection model. The survival rate was from three independent experiments with 10 mice in each group over a 120-h period. Significant differences in adhesion (**A**) and invasion (**B**) were analyzed by a one-way ANOVA test, while zebrafish and mouse infection models (**C**, **D**) were analyzed by a log-rank (Mantel-Cox) test. (*$P < 0.05$; **$P < 0.001$; ***$P < 0.0001$).

MATERIALS AND METHODS

Bacterial strains, plasmids, cell lines, growth conditions and antimicrobials susceptibility testing

A total of 736 lab-owned clinical *Streptococcus* isolates from the National Antimicrobial Resistance Monitoring and Surveillance Program in Animals of China were screened for the presence of SMphages. This included 437 *S. suis*, 74 *S. agalactiae*, and 225 isolates from other *Streptococcus* species, and the SMphage-carrying isolates were subjected to whole genome sequencing (WGS) (Supplementary Table S1). Other strains, plasmids, and cell lines used in experiments are listed in Supplementary Table S3.

Streptococcus strains were grown in Todd-Hewitt broth (THB) or on THB agar plates supplemented with 5% (v/v) newborn calf serum and incubated overnight at 37 °C unless specifically indicated. *Escherichia coli* and *Salmonella enterica* serovar Braenderup strains were grown in Luria-Bertani (LB) broth or on LB agar plates at 37 °C. As needed, antibiotics were added to the media at the following concentrations: 100 μg ml^{-1} erythromycin,

10 μg ml^{-1} tetracycline, 8 μg ml^{-1} florfenicol, 8 μg ml^{-1} tiamulin, 100 μg ml^{-1} spectinomycin, 100 μg ml^{-1} rifampicin, or 100 μg ml^{-1} fusidic acid.

Bovine mammary epithelial cells (BMEC) and human laryngeal carcinoma epithelial cells (HEp-2) were kindly provided by Cell Bank/Stem Cell Bank, Chinese Academy of Sciences. Both cell lines were propagated using Dulbecco's modified Eagle medium (DMEM; Gibco) containing 10% FBS (Gibco) and 1% penicillin plus streptomycin with 5% CO_2 at 37 °C.

Antimicrobial susceptibility testing was performed by broth microdilution method for antimicrobial agents commonly used in veterinary and human medicine (see Table 1) following the methods of CLSI document M100-ED29 [68]. *S. pneumoniae* ATCC 49619 was used for quality control.

Strategy to identify SMphages

A total of 10,983 genome assemblies, including 253 complete genomes and 10,730 WGS sequences from *Streptococcus* species, were retrieved from GenBank (last accessed May 2017). ARGs-carrying prophages (Step 1) and ARGs-associated prophage families (Step2) were characterized by our bidirectional identification strategies (Supplementary Fig. S1A, B). Previously reported SMphages (Φm46.1, Φ10394.4, λSa04, and ΦSsUD.1) were used as reference sequences. We searched for five conserved phage module nucleotides (*orf13-22, orf27-30, orf33-48, orf53-55, orf56-57* of Φm46.1 numbering) in all assemblies of the dataset using a threshold of >50% coverage and >50% nucleotide identity. This procedure returned 531 hits with more than three of the five functional modules (DNA replication, DNA modification, DNA packaging and morphogenesis, host cell lysis, and lysogeny control module). We further delimitated the prophage attachment sites (*attL* and *attR*), and included prophages with attachment sites, ARGs or VFs. The final dataset consisted of 175 SMphages from 171 genomes (Supplementary Fig. S1A and Supplementary Table S1).

We then screened 736 clinical *Streptococcus* isolates for the presence of five conserved phage modules by PCR (Supplementary Table S4; *orf16* for DNA replication, *orf29* for DNA modification, *orf45* for DNA packaging and morphogenesis, *orf54* for host cell lysis, and *intIE* for lysogeny control module). Of these, 102 SMphage-positive strains were identified and subjected to WGS. Finally, a total of 74 SMphages from 69 sequenced clinical isolates were included for further analysis (Supplementary Fig. S1B and Supplementary Table S1).

WGS and phylogenetic analysis

Bacterial genomic DNA was extracted using the E.Z.N.A. Bacterial DNA Kit (Omega Bio-Tek) following the manufacturer's recommendations. The genomic DNA of the SMphage-positive isolates was purified and submitted for WGS using a HiSeq 2000 Sequencing System (Illumina, USA). Draft genomes were assembled with SOAP denovo version 2.04. Assembled contigs were ordered using Mauve v2.4.0. Gaps between the contigs of SMphages were closed by PCR with Sanger sequencing. Complete genomes of the donors and transconjugants in transfer assays were further subjected to long-read sequencing by using a PacBio RSII System (Pacific Biosciences, USA). Complete genomes were assembled preliminarily with SMRT Link v.5.0.1 with PacBio data and were further corrected with WGS Illumina data.

We first obtained the two integrase genes *intIE* (*orf56-57* of Φm46.1) from all SMphages for phylogenetic analysis. The maximum-likelihood (ML) phylogenetic tree was generated using PhyML 3.0 with the neighbor-joining method and bootstrapping for confidence metrics ($N = 1{,}000$). The results were visualized by using FigTree v1.4.2 with a midpoint root method. We then aligned other conserved modules (*orf13-55*) and constructed the prophage core genome phylogenetic tree. A WGS phylogenetic tree was constructed from 244 bacterial genomes carrying prophages. Prophage-host associations based on phage and bacteria genomic phylogenetic analysis were analyzed by using Tanglegram visualization with dendextend (v1.15.2) in R.

Classification of SMphage-encoded ARGs and Alp-Ps

Acquired ARGs were identified using ResFinder with a minimum of 60% coverage and 90% sequence identity [69]. ISs were identified using ISFinder [70]. Transposons were identified by blasting transposase genes against the NCBI nr/nt database. ICEs were predicted by searching type IV secretion system (T4SS) genes and integrases (Ints). The genetic environment of ARGs was further analyzed and visualized using Easyfig 2.2.2.

Putative VFs were screened in SMphage genomes. A total of 127 Alp-Ps were identified by BLASTP comparisons of LPxTG-motif-containing Alp-related proteins in SMphages. A phylogenetic tree was constructed along with reported *alps* genes using the same methods as above. The prevalence, domain features, and repeat regions of each clade of Alp-Ps were further analyzed by CD-Search [71]. The genetic environment of Alp-Ps was further analyzed and visualized using Easyfig 2.2.2.

Prophage integration and excision studies

To identify prophage integration sites, the flanking sequences of 253 SMphages were retrieved and compared with reference genomes of *S. agalactiae* 2603 V/R and *S. suis* P1/7. To test whether the SMphages undergo excision to generate a circular episome under culture conditions, we selected seven representative strains with SMphages integrated at four sites (*rum*, *comEC*, *SAG0725*, and *SAG1105*) from different *Streptococcus* species (Supplementary Table S1). Genomic DNA from overnight bacterial cultures was extracted as the template for PCR amplification. A PCR strategy was designed to detect the SMphage integration and excision using primer pairs (Supplementary Table S4): integrated form, *attL* (P1 + P2) and *attR* (P3 + P4); excision or empty form, *attB* (P1 + P4); and circular episome from, *attP* (P2 + P3). PCR products were further subjected to Sanger sequencing. Putative *att* site consensus sequences were retrieved from alignments by using MEGA 7. The nucleotide difference of the *attP*, *attL* and *attR* sequences was compared with corresponding *attB* sequences. The size of each prophage was then calculated after the precise delimitation of prophages.

Bacteria construction

The ICE*Su*AKJ18_*rum* deletion mutant was generated by a previously described procedure [72]. Briefly, the upstream and downstream fragments of ICE were amplified from *S. suis* AKJ18. The two purified fragments were then integrated into the pre-linearized temperature sensitive vector pSET4s via *In Fusion*, and the resulting recombinant vector pSET4s::ICE was transformed into *E. coli* DH5α for propagation and verification, followed by electrotransformation into *S. suis* AKJ18 competent cells. Mutant strains (AKJ18ΔICE) were selected on THB agar for their sensitivity to spectinomycin and verified by PCR and Sanger sequencing. The *alp*-Ps gene deletion mutants of *S. agalactiae* strains were constructed by the same protocol using the primers in Supplementary Table S4.

The *alp*-Ps complementation vectors were constructed using the shuttle cloning vector pSET2 [73]. A fragment containing the complete open reading frame (ORF) of the *alp*-Ps gene was amplified from the genome and ligated into the pSET2 vector. The recombinant vector was transformed into *E. coli* DH5α for propagation prior to electrotransformation of the Δ*alp*-Ps mutants. Complementation vector-transformed Δ*alp*-Ps mutants were grown on THB agar containing spectinomycin and verified by PCR and Sanger sequencing.

Prophage induction and transmission electron microscopy

The prophage induction assay was performed as previously described [74, 75], with minor modifications. Briefly, an early-exponential-phase culture ($OD_{600} = 0.2$) of *Streptococcus* strains carrying SMphages was treated with mitomycin C (MMC) at a final concentration of 0.5 μg ml^{-1} for overnight. Cells and debris were removed by centrifugation, and the supernatants were filtered (0.45 μm). Supernatants were treated with 0.125% Triton X-100 for 30 min at 37 °C to lyse outer membrane vesicles, and were then treated with DNase I (1 μg ml^{-1}, final concentration) and RNase A (1 μg ml^{-1}, final concentration) to remove exogenous nucleic acids. Next, the phage particles were collected by NaCl and PEG8000 precipitation. The resulting pellet was resuspended in SM buffer (0.15 M NaCl, 5 mM $MgCl_2$, 1 mM $CaCl_2$, 10 mM Tris HCl, pH 7.5) and subjected to CsCl centrifugation [74]. The purified phage particles were enriched in a band of the second CsCl step. Phage particles were negatively stained with 2% phosphotungstic acid and observed through a transmission electron microscope at an accelerating voltage of 80 kV.

Overnight bacterial cultures were diluted 1:100 into fresh THB and grown at 37 °C with shaking at 200 r.p.m. until $OD_{600} = 0.5$. Cultures were treated with or without MMC (0.5 μg ml^{-1}, final concentration) for 1 h, prior to bacterial DNA extraction. The extracted DNA was used as the template for transformation experiments. Phage genomic DNA was extracted using a phenol: chloroform extraction method. Briefly, purified phage particles were treated with a proteinase K cocktail (50 μg ml^{-1} proteinase K, 20 mM EDTA, and 0.5% SDS, final concentration) at 55 °C for 3 h. The mixture was cooled to room temperature, and the aqueous layer was reextracted twice with an equal volume of phenol/chloroform/isoamylalcohol (25:24:1) and once with an equal volume of chloroform. The aqueous phase was precipitated with 1/10 volume of 3 M NaOAc (pH 7.0) and 2.5 volumes of

ice-cold ethanol for 2 hours at −20 °C. Finally, the pellet was washed with 70% ethanol and resuspended in ultrapure water. The purified phage DNA was used as the template for transformation experiments.

Plaque forming assay and transduction

A total of 45 SMphage-negative clinical isolates (30 *S. suis* including *S. suis* P1/7RF, 10 *S. agalactiae*, and 5 *S. dysgalactiae*) were used as phage-infected recipients. The SMphage titer in all samples was determined by qPCR. Sandwich plaque assays were performed as described previously [75]. Briefly, overnight recipient cultures were diluted 1:100 into fresh THB and grown to an $OD_{600} = 0.4–0.5$. Phage particles were added to the bacterial culture and further incubated for 15 min at 37 °C. The mixed culture was then poured into 5 ml molten THA with 0.5% agar and spread onto THA plates. The plates were incubated overnight at 37 °C for plaque formation. For phage transduction, 100 µl of the mixed culture was plated onto THA plates containing appropriate antibiotics and incubated overnight at 37 °C to select transductants. Five biological replicates and three technical replicates were used in this experiment.

Transformation experiments

Natural transformation experiments were performed as described previously [76, 77]. For these procedures, *S. suis* develops natural competence when exposed to a peptide pheromone. The amino acid sequences of pheromones ComR and ComS in *S. suis* P1/7 (Accession No.: NC_012925.1) were obtained from the NCBI database. Peptide pheromones were synthesized at a purity grade of >95% (Genscript Biotech, China). Stock solutions were dissolved to a final concentration of 5 mM with ultrapure water and stored at −70 °C. *S. suis* strain P1/7RF was grown in THB at 37 °C until $OD_{600} = 0.6$. The culture was added to pre-warmed THB at 1:50 and grown without shaking until $OD_{600} = 0.03–0.05$. An aliquot (100 µl) of culture was removed and 5 µl of peptide pheromone was added (for a final concentration of 250 µM) along with the DNA template. After 2 h incubation without shaking, the culture was spread onto THA plates containing appropriate antibiotics. Three biological replicates and three technical replicates were used in this experiment.

Electroporation experiments were performed as described previously [76]. Briefly, an aliquot (100 µl) of *Streptococcus* competent cell suspension was mixed with 10 µl of template DNA and placed in a prechilled sterile electroporation cuvette (2 mm electrode gap, BTX-Harvard Apparatus, Holliston MA, USA) and hold on ice for 30 min. The electroporation transformation was performed using an ECM 399 Electroporation System (2.5 kV, 200 Ω, and 25µF). The mixture was diluted with prewarmed THY broth containing 10% sucrose and 10 mM $MgCl_2$ and incubated at 37 °C for 4 h. The cells were spread on THA plate containing appropriate antibiotics and incubated overnight. Three biological replicates were used in this experiment.

Filter mating experiments

Four strains were used as donors (i.e., *S. dysgalactiae* DY107 and *S. suis* AKJ18, NJ3, and SS389) (Supplementary Table S2), and *S. suis* P1/7RF (rifampicin and fusidic acid resistance) was used as recipient. Filter mating experiments were performed as described previously [78]. In brief, donor and recipient strains were mixed at a ratio of 1:10, then the mixtures were washed three times with PBS and treated with Triton X-100 or Triton X-100/DNase I. Subsequently, the mixtures were centrifuged and resuspended with THB and placed on a nitrocellulose membrane on THA plates (incubated at 37 °C for 8 h). Bacteria were recovered from membranes by washing THA plates with THB containing appropriate antibiotics. Three biological replicates and three technical replicates were adopted for each treatment. The transconjugants were further confirmed by PCR using specific primers, pulsed-field gel electrophoresis (PFGE) and Southern blot, and WGS.

PFGE and Southern blot

PFGE was performed as previously described [79, 80]. To determine the location of SMphages and ARGs, genomic DNA from four of the donors, the recipients, and the corresponding transconjugants were digested with SmaI endonuclease and subjected to PFGE. Electrophoresis was carried out at 14 °C and 6 V cm^{-1} for 22.2 h, with an initial pulse time of 1.2 s and a final pulse time of 30 s, by using a CHEF-DR II system (Bio-Rad Laboratories). A *Salmonella enterica* serovar Braenderup strain (H9812) digested with XbaI was used for molecular weight and size standard. For Southern blot, DNA fragments of ARGs carried by SMphage in corresponding strains were then labeled with digoxigenin to be used as probes. Southern blot was completed using DIG High Prime DNA Labeling and Detection Starter Kit I (Roche, USA) according to the manufacturer's protocol. Primers used for Southern blot hybridization are shown in Supplementary Table S4. The images were analyzed using Bio-Rad Gel Doc XR+ Imaging System.

Growth curve and competition assays

The fitness difference between transconjugants and recipients was investigated by in vitro growth and competition assays as described previously [78, 81]. For in vitro growth assays, the mid-log growth phase cultures (donors, recipient, and transconjugants) were adjusted to the same OD and diluted by a factor of 1:100 into fresh THB supplemented with 0.2% (g/v) yeast extract. OD measurements at a wavelength of 600 nm were performed in a 96-well plate using a spectrophotometer (Bio-Rad, USA) at 15 min intervals for 12 h. The experiments were repeated three times. For in vitro competition assays, bacterial cultures (recipient and transconjugants) were adjusted to $OD_{600} = 0.1$, mixed at a 1:1 ratio, and inoculated at a 1:100 ratio into 10 mL fresh THB at 37 °C with shaking at 200 r.p.m for 24 h. The mixtures at both the start point (0 h) and endpoint (24 h) were plated on THA plates without or with corresponding antibiotics and incubated at 37 °C for 48 h. The relative fitness (w) was calculated in competition experiments as previously described [81]. The experiments were repeated 10 times.

Effects of MMC on bacterial growth and prophage excision

To examine growth dynamics during prophage induction, the mid-log growth phase cultures were adjusted to the same OD and diluted by a factor of 1:100 into fresh THB supplemented with 0.2% (g/v) yeast extract. After 2 h, MMC was added to the cultures at a final concentration of 0, 0.05, and 0.5 µg ml^{-1}. OD measurements at a wavelength of 600 nm were performed in a 96-well plate using a spectrophotometer (Bio-Rad, USA). The cultures were incubated and continued and the OD_{600} was monitored until 12 hours.

Overnight bacterial cultures were diluted 1:100 into fresh THB and grown at 37 °C until $OD_{600} = 0.5$. Then, MMC was added to a final concentration of 0, 0.05 µg ml^{-1}, or 0.5 µg ml^{-1}, and the cultures were incubated for 1 h in the dark. Total DNA was extracted using the E.Z.N.A. Bacterial DNA Kit (Omega Bio-Tek, USA) according to the instructions of the kit. DNA concentration was measured using NanoDrop 2000 (ThermoFisher, USA) and adjusted to the same concentration as the PCR templates. PCR amplification was used to detect changes in prophage excision and circularization in donors and transconjugants, and ImageJ v1.46r [82] was used to analyze the density of electrophoretic bands on an agar gel.

Cell adhesion and invasions assays

To understand the functions of Alp-Ps, we constructed the *alp*-P deletion strains Δ*alp*-P1 and Δ*alp*-P2, and complement strains CΔ*alp*-P1and CΔ*alp*-P2 in *S. agalactiae* strains G1-9 and GD201008-001, respectively. Bacterial adhesion and invasion assays were performed as described [83], modified to some extent. Briefly, BMEC and HEp-2 cells were both grown in DMEM containing 10% FBS at 37 °C with 5% CO_2 for 12-16 h to obtain monolayer cells in a 24-well microtiter plate. Bacteria were grown to the mid-log phase, washed twice with sterile PBS, and then added to confluent monolayers at a multiplicity of infection (MOI) of 100 and centrifuged for 5 minutes at 211 x *g* to synchronize infection. After a 2-h incubation, monolayers were extensively washed three times with PBS to remove the non-adherent bacteria, lysed, and plated on THA for CFU counts. For the invasion assay, the monolayers using the same treatment as above were further incubated for 1 h before cell lysis with a medium supplemented with penicillin and streptomycin (200 units ml^{-1} and 200 µg ml^{-1}, respectively) to kill extracellular bacteria. Bacterial adhesion and invasion were calculated as follows: recovered CFU/initial inoculum CFU×100. Three biological replicates and three technical replicates were used in this experiment.

Animal models

The zebrafish infection experiments were carried out as previously reported [84]. Before being injected into the zebrafish, bacterial cultures (*S. agalactiae* strains G1-9, Δ*alp*-P1, CΔ*alp*-P1, GD201008-001, Δ*alp*-P2, and CΔ*alp*-P2) in the mid-log growth phase were washed twice in PBS and adjusted to appropriate doses (CFU per fish). Zebrafish were anesthetized with tricaine methanesulfonate (MS-222) and were then intraperitoneally injected with 20 µl of 10-fold serially diluted suspensions of bacteria. Each treatment group included 15 zebrafish, incubated in plastic containers for

120 h at 28 °C, and the mortality was monitored in three parallel experiments. Fish in the control group were injected with an equal volume of PBS. The 50% lethal dose (LD_{50}) values were calculated by the Reed-Muench method [85].

Male ICR mice (4-5 weeks of age) were purchased from the Experimental Animal Center, Yangzhou University. To assess potential virulence, mice were divided into six groups (six *Streptococcus* strains, G1-9, Δ*alp*-P1, CΔ*alp*-P1, GD201008-001, Δ*alp*-P2, and CΔ*alp*-P2) and each group was further divided into two subgroups (two concentrations, 10^6–10^7 CFU per mouse of G1-9 and its derivants or 10^1–10^2 CFU per mouse in GD201008-001 and its derivants, $n = 10$ mice for each treatment group). Mid-log growth phase bacteria were washed twice in PBS and adjusted to appropriate doses (CFU per mouse). All experimental groups were injected intraperitoneally with 100 µl of the 10-fold-diluted bacterial suspension. The control group was injected with 100 µl PBS. For the infection experiment, groups of five mice were intraperitoneally infected with matched inocula in a predetermined dose of 5×10^7 CFU per mouse in strain G1-9 and its derivants or 5×10^2 CFU per mouse in strain GD201008-001 and its derivants. The control group was injected with PBS. Samples were taken at 16 h post-infection. Blood was collected and the livers, spleens, and brains were obtained aseptically. The organs (0.05 g per organ) were trimmed, placed in 500 µl of PBS, and homogenized in a high-speed homogenizer. Then the homogenate and blood samples in PBS were spread by serial dilution onto THA plates and incubated overnight at 37 °C. Colonies were counted and expressed as CFU g^{-1} for organ samples or CFU ml^{-1} for blood samples.

Statistical analysis

Statistical analysis was performed using SPSS 20.0, and graphs were generated using GraphPad Prism 7 and R. All experiments were repeated at least in triplicate, and the values were presented as the mean ± standard deviation. A one-way ANOVA was used in the analysis of the transfer assay, cell adhesion and invasion, and mouse systemic infection, and a log-rank (Mantel-Cox) test was used in the analysis of the survival curves of zebrafish and mouse infection models. Differences among the groups were considered statistically significant with $P < 0.05$.

DATA AVAILABILITY

All data are available in the main text or the supplementary materials.

REFERENCES

1. Feiner R, Argov T, Rabinovich L, Sigal N, Borovok I, Herskovits AA. A new perspective on lysogeny: prophages as active regulatory switches of bacteria. Nat Rev Microbiol. 2015;13:641–50.
2. Howard-Varona C, Hargreaves KR, Abedon ST, Sullivan MB. Lysogeny in nature: mechanisms, impact and ecology of temperate phages. ISME J. 2017;11:1511–20.
3. Penades JR, Chen J, Quiles-Puchalt N, Carpena N, Novick RP. Bacteriophage-mediated spread of bacterial virulence genes. Curr Opin Microbiol. 2015;23:171–8.
4. Brussow H, Canchaya C, Hardt WD. Phages and the evolution of bacterial pathogens: from genomic rearrangements to lysogenic conversion. Microbiol Mol Biol Rev. 2004;68:560–602.
5. Davies EV, Winstanley C, Fothergill JL, James CE. The role of temperate bacteriophages in bacterial infection. FEMS Microbiol Lett. 2016;363:fnw015.
6. Wagner PL, Waldor MK. Bacteriophage control of bacterial virulence. Infect Immun. 2002;70:3985–93.
7. Marti E, Variatza E, Balcazar JL. Bacteriophages as a reservoir of extended-spectrum beta-lactamase and fluoroquinolone resistance genes in the environment. Clin Microbiol Infect. 2014;20:O456–9.
8. Modi SR, Lee HH, Spina CS, Collins JJ. Antibiotic treatment expands the resistance reservoir and ecological network of the phage metagenome. Nature. 2013;499:219–22.
9. Enault F, Briet A, Bouteille L, Roux S, Sullivan MB, Petit MA. Phages rarely encode antibiotic resistance genes: a cautionary tale for virome analyses. ISME J. 2017;11:237–47.
10. Lekunberri I, Subirats J, Borrego CM, Balcazar JL. Exploring the contribution of bacteriophages to antibiotic resistance. Environ Pollut. 2017;220:981–4.
11. Ubukata K, Konno M, Fujii R. Transduction of drug resistance to tetracycline, chloramphenicol, macrolides, lincomycin and clindamycin with phages induced from *Streptococcus pyogenes*. J Antibiot. 1975;28:681–8.
12. Mazaheri Nezhad Fard R, Barton MD, Heuzenroeder MW. Bacteriophage-mediated transduction of antibiotic resistance in enterococci. Lett Appl Microbiol. 2011;52:559–64.
13. Torres-Barcelo C. The disparate effects of bacteriophages on antibiotic-resistant bacteria. Emerg Microbes Infect. 2018;7:168.
14. Haenni M, Lupo A, Madec JY. Antimicrobial resistance in *Streptococcus* spp. Microbiol Spectr. 2018;6. https://doi.org/10.1128/microbiolspec.arba-0008-2017.
15. Krzysciak W, Pluskwa KK, Jurczak A, Koscielniak D. The pathogenicity of the *Streptococcus* genus. Eur J Clin Microbiol Infect Dis. 2013;32:1361–76.
16. CDC. Antibiotic resistance threats in the United States, 2019. Atlanta, GA: U.S. Department of Health and Human Services, CDC 2019.
17. Huang J, Ma J, Shang K, Hu X, Liang Y, Li D, et al. Evolution and diversity of the antimicrobial resistance associated mobilome in *Streptococcus suis*: a probable mobile genetic elements reservoir for other streptococci. Front Cell Infect Microbiol. 2016;6:118.
18. Palmieri C, Varaldo PE, Facinelli B. *Streptococcus suis*, an emerging drug-resistant animal and human pathogen. Front Microbiol. 2011;2:235.
19. Baquero F, Martínez JL, Lanza VF, Rodríguez-Beltrán J, Galán JC, San Millán A, et al. Evolutionary pathways and trajectories in antibiotic resistance. Clin Microbiol Rev. 2021;34:e0005019.
20. Arnold BJ, Huang IT, Hanage WP. Horizontal gene transfer and adaptive evolution in bacteria. Nat Rev Microbiol. 2022;20:206–18.
21. Partridge SR, Kwong SM, Firth N, Jensen SO. Mobile genetic elements associated with antimicrobial resistance. Clin Microbiol Rev. 2018;31:e00088–17.
22. Libante V, Nombre Y, Coluzzi C, Staub J, Guedon G, Gottschalk M, et al. Chromosomal conjugative and mobilizable elements in *Streptococcus suis*: major actors in the spreading of antimicrobial resistance and bacteriocin synthesis genes. Pathogens 2019;9:22.
23. Varaldo PE, Montanari MP, Giovanetti E. Genetic elements responsible for erythromycin resistance in streptococci. Antimicrob Agents Chemother. 2009;53:343–53.
24. Ambroset C, Coluzzi C, Guédon G, Devignes MD, Loux V, Lacroix T, et al. New insights into the classification and integration specificity of *Streptococcus* integrative conjugative elements through extensive genome exploration. Front Microbiol. 2015;6:1483.
25. Wozniak RA, Waldor MK. Integrative and conjugative elements: mosaic mobile genetic elements enabling dynamic lateral gene flow. Nat Rev Microbiol. 2010;8:552–63.
26. Ramsay JP, Firth N. Diverse mobilization strategies facilitate transfer of non-conjugative mobile genetic elements. Curr Opin Microbiol. 2017;38:1–9.
27. Guédon G, Libante V, Coluzzi C, Payot S, Leblond-Bourget N. The obscure world of integrative and mobilizable elements, highly widespread elements that pirate bacterial conjugative systems. Genes 2017;8:337.
28. Di Luca MC, D'Ercole S, Petrelli D, Prenna M, Ripa S, Vitali LA. Lysogenic transfer of *mef*(A) and *tet*(O) genes carried by Φm46.1 among group A streptococci. Antimicrob Agents Chemother. 2010;54:4464–6.
29. Chen J, Quiles-Puchalt N, Chiang YN, Bacigalupe R, Fillol-Salom A, Chee MSJ, et al. Genome hypermobility by lateral transduction. Science 2018;362:207–12.
30. Fillol-Salom A, Bacigalupe R, Humphrey S, Chiang YN, Chen J, Penades JR. Lateral transduction is inherent to the life cycle of the archetypical *Salmonella* phage P22. Nat Commun. 2021;12:6510.
31. Keen EC, Bliskovsky VV, Malagon F, Baker JD, Prince JS, Klaus JS, et al. Novel "superspreader" bacteriophages promote horizontal gene transfer by transformation. mBio 2017;8:e02115–16.
32. Haaber J, Leisner JJ, Cohn MT, Catalan-Moreno A, Nielsen JB, Westh H, et al. Bacterial viruses enable their host to acquire antibiotic resistance genes from neighbouring cells. Nat Commun. 2016;7:13333.
33. Garcia-Aljaro C, Balleste E, Muniesa M. Beyond the canonical strategies of horizontal gene transfer in prokaryotes. Curr Opin Microbiol. 2017;38:95–105.
34. Brabban AD, Hite E, Callaway TR. Evolution of foodborne pathogens via temperate bacteriophage-mediated gene transfer. Foodborne Pathog Dis. 2005;2:287–303.
35. Brenciani A, Bacciaglia A, Vignaroli C, Pugnaloni A, Varaldo PE, Giovanetti E. Φm46.1, the main *Streptococcus pyogenes* element carrying *mef*(A) and *tet*(O) genes. Antimicrob Agents Chemother. 2010;54:221–9.
36. Banks DJ, Porcella SF, Barbian KD, Martin JM, Musser JM. Structure and distribution of an unusual chimeric genetic element encoding macrolide resistance in phylogenetically diverse clones of group A *Streptococcus*. J Infect Dis. 2003;188:1898–908.
37. Tettelin H, Masignani V, Cieslewicz MJ, Donati C, Medini D, Ward NL, et al. Genome analysis of multiple pathogenic isolates of *Streptococcus agalactiae*: implications for the microbial "pan-genome". Proc Natl Acad Sci Usa 2005;102:13950–5.
38. Palmieri C, Princivalli MS, Brenciani A, Varaldo PE, Facinelli B. Different genetic elements carrying the *tet*(W) gene in two human clinical isolates of *Streptococcus suis*. Antimicrob Agents Chemother. 2011;55:631–6.
39. D'Ercole S, Petrelli D, Prenna M, Zampaloni C, Catania MR, Ripa S, et al. Distribution of *mef*(A)-containing genetic elements in erythromycin-resistant isolates of *Streptococcus pyogenes* from Italy. Clin Microbiol Infect. 2005;11:927–30.
40. Dion MB, Oechslin F, Moineau S. Phage diversity, genomics and phylogeny. Nat Rev Microbiol. 2020;18:125–38.

41. Du FS, Lv X, Duan D, Wang LP, Huang JH. Characterization of a linezolid- and vancomycin-resistant *Streptococcus suis* isolate that harbors *optrA* and *vanG* operons. Front Microbiol. 2019;10:2026.
42. Varhimo E, Savijoki K, Jalava J, Kuipers OP, Varmanen P. Identification of a novel streptococcal gene cassette mediating SOS mutagenesis in *Streptococcus uberis*. J Bacteriol. 2007;189:5210–22.
43. Srinivasan V, Metcalf BJ, Knipe KM, Ouattara M, McGee L, Shewmaker PL, et al. *vanG* element insertions within a conserved chromosomal site conferring vancomycin resistance to *Streptococcus agalactiae* and *Streptococcus anginosus*. mBio 2014;5:e01386–14.
44. Johnston C, Martin B, Fichant G, Polard P, Claverys JP. Bacterial transformation: distribution, shared mechanisms and divergent control. Nat Rev Microbiol. 2014;12:181–96.
45. Liu Y, Zeng Y, Huang Y, Gu L, Wang S, Li C, et al. HtrA-mediated selective degradation of DNA uptake apparatus accelerates termination of pneumococcal transformation. Mol Microbiol. 2019;112:1308–25.
46. Giovanetti E, Brenciani A, Morroni G, Tiberi E, Pasquaroli S, Mingoia M, et al. Transduction of the *Streptococcus pyogenes* bacteriophage Φm46.1, carrying resistance genes *mef*(A) and *tet*(O), to other *Streptococcus* species. Front Microbiol. 2014;5:746.
47. Zabriskie JB. The role of temperate bacteriophage in the production of erythrogenic toxin by group A streptococci. J Exp Med. 1964;119:761–80.
48. Steinmoen H, Knutsen E, Havarstein LS. Induction of natural competence in *Streptococcus pneumoniae* triggers lysis and DNA release from a subfraction of the cell population. Proc Natl Acad Sci Usa 2002;99:7681–6.
49. Creti R, Baldassarri L, Montanaro L, Arciola CR. The alpha-like surface proteins: an example of an expanding family of adhesins. Int J Artif Organs. 2008;31:834–40.
50. Li J, Kasper DL, Ausubel FM, Rosner B, Michel JL. Inactivation of the alpha C protein antigen gene, *bca*, by a novel shuttle/suicide vector results in attenuation of virulence and immunity in group B *Streptococcus*. Proc Natl Acad Sci Usa 1997;94:13251–6.
51. Stålhammar-Carlemalm M, Areschoug T, Larsson C, Lindahl G. The R28 protein of *Streptococcus pyogenes* is related to several group B streptococcal surface proteins, confers protective immunity and promotes binding to human epithelial cells. Mol Microbiol. 1999;33:208–19.
52. Creti R, Imperi M, Baldassarri L, Pataracchia M, Alfarone G, Orefici G. Lateral transfer of alpha-like protein gene cassettes among streptococci: identification of a new family member in *Streptococcus dysgalactiae* subsp. *equisimilis*. Lett Appl Microbiol. 2007;44:224–7.
53. Liu G, Zhang W, Lu C. Complete genome sequence of *Streptococcus agalactiae* GD201008-001, isolated in China from tilapia with meningoencephalitis. J Bacteriol. 2012;194:6653.
54. Balcazar JL. Bacteriophages as vehicles for antibiotic resistance genes in the environment. PLoS Pathog. 2014;10:e1004219.
55. Abedon ST, Lejeune JT. Why bacteriophage encode exotoxins and other virulence factors. Evol Bioinform Online. 2007;1:97–110.
56. Allen HK, Looft T, Bayles DO, Humphrey S, Levine UY, Alt D, et al. Antibiotics in feed induce prophages in swine fecal microbiomes. mBio. 2011;2:e00260–11.
57. Gabashvili E, Osepashvili M, Koulouris S, Ujmajuridze L, Tskhitishvili Z, Kotetishvili M. Phage transduction is involved in the intergeneric spread of antibiotic resistance-associated bla_{CTX-M}, *mel*, and *tetM* loci in natural populations of some human and animal bacterial pathogens. Curr Microbiol. 2020;77:185–93.
58. Coluzzi C, Guédon G, Devignes MD, Ambroset C, Loux V, Lacroix T, et al. A glimpse into the world of integrative and mobilizable elements in streptococci reveals an unexpected diversity and novel families of mobilization proteins. Front Microbiol. 2017;8:443.
59. Maeland JA, Afset JE, Lyng RV, Radtke A. Survey of immunological features of the alpha-like proteins of *Streptococcus agalactiae*. Clin Vaccin Immunol. 2015;22:153–9.
60. Lindahl G, Stålhammar-Carlemalm M, Areschoug T. Surface proteins of *Streptococcus agalactiae* and related proteins in other bacterial pathogens. Clin Microbiol Rev. 2005;18:102–27.
61. Darmancier H, Domingues CPF, Rebelo JS, Amaro A, Dionisio F, Pothier J, et al. Are virulence and antibiotic resistance genes linked? A comprehensive analysis of bacterial chromosomes and plasmids. Antibiotics (Basel). 2022;11:706.
62. Katayama Y, Ito T, Hiramatsu K. A new class of genetic element, *Staphylococcus* cassette chromosome *mec*, encodes methicillin resistance in *Staphylococcus aureus*. Antimicrob Agents Chemother. 2000;44:1549–55.
63. Novick RP, Christie GE, Penades JR. The phage-related chromosomal islands of Gram-positive bacteria. Nat Rev Microbiol. 2010;8:541–51.
64. Guglielmini J, Quintais L, Garcillan-Barcia MP, de la Cruz F, Rocha EPC. The repertoire of ICE in prokaryotes underscores the unity, diversity, and ubiquity of conjugation. PLoS Genet. 2011;7:e1002222.
65. Daccord A, Ceccarelli D, Burrus V. Integrating conjugative elements of the SXT/R391 family trigger the excision and drive the mobilization of a new class of *Vibrio* genomic islands. Mol Microbiol. 2010;78:576–88.
66. Waldor MK. Mobilizable genomic islands: going mobile with *oriT* mimicry. Mol Microbiol. 2010;78:537–40.
67. Huang J, Liang Y, Guo D, Shang K, Ge L, Kashif J, et al. Comparative genomic analysis of the ICE*Sa*2603 family ICEs and spread of *erm*(B)- and *tet*(O)-carrying transferable 89K-subtype ICEs in swine and bovine isolates in China. Front Microbiol. 2016;7:55.
68. CLSI. Performance Standards for Antimicrobial Susceptibility Testing. 33rd ed. CLSI supplement M100.: Wayne, PA: Clinical and Laboratory Standards Institute; 2023.
69. Zankari E, Hasman H, Cosentino S, Vestergaard M, Rasmussen S, Lund O, et al. Identification of acquired antimicrobial resistance genes. J Antimicrob Chemother. 2012;67:2640–4.
70. Siguier P, Perochon J, Lestrade L, Mahillon J, Chandler M. ISfinder: the reference centre for bacterial insertion sequences. Nucleic Acids Res. 2006;34:D32–6.
71. Marchler-Bauer A, Bryant SH. CD-Search: protein domain annotations on the fly. Nucleic Acids Res. 2004;32:W327–31.
72. Takamatsu D, Osaki M, Sekizaki T. Thermosensitive suicide vectors for gene replacement in *Streptococcus suis*. Plasmid 2001;46:140–8.
73. Takamatsu D, Osaki M, Sekizaki T. Construction and characterization of *Streptococcus suis-Escherichia coli* shuttle cloning vectors. Plasmid 2001;45:101–13.
74. Bensing BA, Siboo IR, Sullam PM. Proteins PblA and PblB of *Streptococcus mitis*, which promote binding to human platelets, are encoded within a lysogenic bacteriophage. Infect Immun. 2001;69:6186–92.
75. Tang F, Bossers A, Harders F, Lu C, Smith H. Comparative genomic analysis of twelve *Streptococcus suis* (pro)phages. Genomics 2013;101:336–44.
76. Zhu Y, Dong W, Ma J, Zhang Y, Pan Z, Yao H. Utilization of the ComRS system for the rapid markerless deletion of chromosomal genes in *Streptococcus suis*. Future Microbiol. 2019;14:207–22.
77. Zaccaria E, van Baarlen P, de Greeff A, Morrison DA, Smith H, Wells JM. Control of competence for DNA transformation in *Streptococcus suis* by genetically transferable pherotypes. PLoS One. 2014;9:e99394.
78. Chen L, Huang JH, Huang XX, He YP, Sun JJ, Dai XY, et al. Horizontal transfer of different *erm*(B)-carrying mobile elements among *Streptococcus suis* strains with different serotypes. Front Microbiol. 2021;12:628740.
79. Vela AI, Goyache J, Tarradas C, Luque I, Mateos A, Moreno MA, et al. Analysis of genetic diversity of *Streptococcus suis* clinical isolates from pigs in Spain by pulsed-field gel electrophoresis. J Clin Microbiol. 2003;41:2498–502.
80. Huang JH, Shang KX, Kashif J, Wang LP. Genetic diversity of *Streptococcus suis* isolated from three pig farms of China obtained by acquiring antibiotic resistance genes. J Sci Food Agr. 2015;95:1454–60.
81. Kodio O, Georges Togo AC, Sadio Sarro YD, Fane B, Diallo F, Somboro A, et al. Competitive fitness of *Mycobacterium tuberculosis* in vitro. Int J Mycobacteriol. 2019;8:287–91.
82. Rasband WS. ImageJ, U. S. National Institutes of Health, Bethesda, Maryland, USA. https://imagej.net/ij/index.html. 1997.
83. Deshayes de Cambronne R, Fouet A, Picart A, Bourrel AS, Anjou C, Bouvier G, et al. CC17 group B *Streptococcus* exploits integrins for neonatal meningitis development. J Clin Investig. 2021;131:e136737.
84. Neely MN, Pfeifer JD, Caparon M. *Streptococcus*-zebrafish model of bacterial pathogenesis. Infect Immun. 2002;70:3904–14.
85. Reed LJ, Muench H. A simple method of estimating fifty per cent endpoints. Am J Epidemiol. 1938;27:493–7.

ACKNOWLEDGEMENTS

This work was supported by the National Key R&D Program of China (2022YFD1800400), the National Natural Science Foundation of China (32172917, 32072915 and 31872517), the Natural Science Foundation of Jiangsu Province (BK20170710 and BK20210402), the Jiangsu Agriculture Science and Technology Innovation Fund (CX(22)3039), the Jiangsu Distinguished Professor Program (060804097), the Distinguished Young Scholars of the National Natural Science Foundation of China (Overseas), and the Priority Academic Program Development of Jiangsu Higher Education Institutions (PAPD). The bioinformatics analyses were supported by the high-performance computing platform of Bioinformatics Center, Nanjing Agricultural University, and a startup award at Nanjing Agricultural University 060804009).

We would like to thank Dr. Zongfu Wu and Jiale Ma from Nanjing Agricultural University for their assistance in the bacterial virulence study, and Dr. Qijing Zhang from Iowa State University for fruitful discussions and manuscript improvement.

AUTHOR CONTRIBUTIONS

JH and LW conceived and designed the experiments. JH, ZW, JL, YT, WZ and XH performed bioinformatics analyses. JH, XD, JS, PH and JZ generated strains and plasmids and performed HGT and other experiments. XD, GL and XW performed the cell and animal experiments. JH, XD and ZW wrote the original draft. LW, JL, DRC, YW and SM reviewed and edited the manuscript.

COMPETING INTERESTS

The authors declare no competing interests.

ETHICS STATEMENT

Animal experiments were carried out at the Laboratory Animal Center of Nanjing Agricultural University, according to the guidelines of Experimental Animal Management Measures of Jiangsu Province and were approved by the Laboratory Animal Monitoring Committee of Jiangsu Province, China [Permit number: SYXK (Su) 2017-0007].

ADDITIONAL INFORMATION

Supplementary information The online version contains supplementary material available at https://doi.org/10.1038/s41396-023-01463-4.

Correspondence and requests for materials should be addressed to Jinxin Liu or Liping Wang.